Light-front versus equal-time quantization in ϕ^4 theory[a]

S.S. Chabysheva

Department of Physics and Astronomy
University of Minnesota-Duluth
Duluth, Minnesota 55812

(Dated: December 13, 2016)

Abstract

There is a discrepancy between light-front and equal-time values for the critical coupling of two-dimensional ϕ^4 theory. A proposed resolution is to take into account the difference between mass renormalizations in the two quantizations. This distinction was first discussed by M. Burkardt. It prevents direct comparison of bare parameters; however, a method proposed here allows calculation of the difference and thereby resolves the discrepancy. We also consider the consequences of allowing a sector-dependent constituent mass.

arXiv:1612.03419v1 [hep-th] 11 Dec 2016

[a] Based on a talk contributed to the Lightcone 2016 workshop, Lisbon, Portugal, September 5-8, 2016.

I. INTRODUCTION

Previous calculations [1, 2] have shown that there is a systematic difference between light-front and equal-time values for the critical coupling of ϕ^4 theory. Here we discuss the resolution of this by considering the difference in mass renormalizations as originally suggested by Burkardt [3]. However, we also show that the expected behavior of the probability for higher Fock sectors, that they should grow dramatically as the critical coupling is approached, is not observed. This interferes with the estimation of the mass renormalization. As a means to resolve this, we consider use of sector-dependent constituent mass in the solution of the Hamiltonian eigenvalue problem. Many of the details of the methods used, particularly for this eigenvalue problem, are presented by Hiller [4].

Our light-front estimate of the critical coupling is based on calculations of the lowest massive eigenstates as a function of the coupling for both the odd and even sectors. The values of the eigenmass squared are plotted in Fig. 1. The intersections of the spectra with

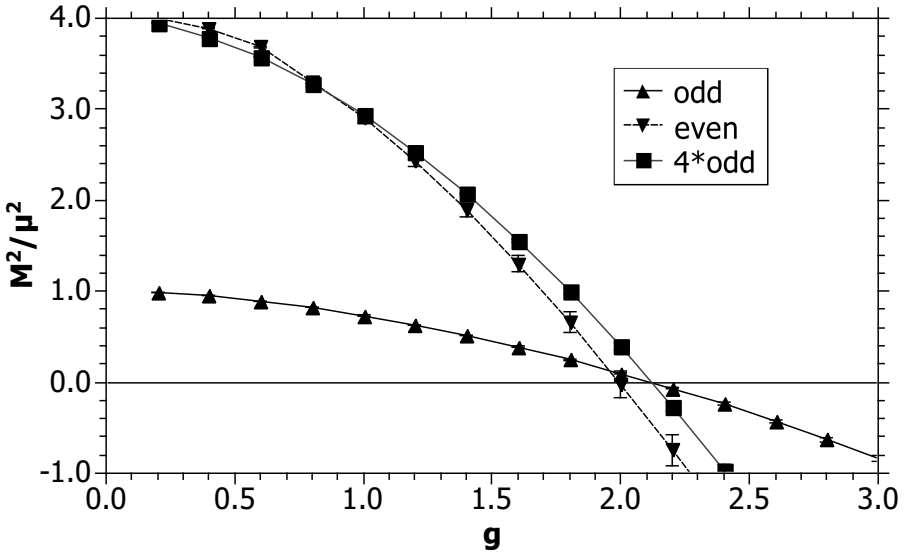

FIG. 1. The lowest masses for the odd and even eigenstates of ϕ^4 theory, from [1]. The threshold for two-particle states, at four times the mass-squared of the odd case, is also shown.

zero indicate a critical coupling of $g = 2.1 \pm 0.05$. This value is compared with values from other calculations in Table I.

There is clearly a systematic difference between results for light-front quantization and equal-time quantization. In the following section we describe the resolution of this difference in terms of a shift in the effective constituent mass. We also discuss, in Sec. III, the implementation of a sector-dependent constituent mass as an attempt to improve the calculation of the shift. A summary is given in Sec. IV.

II. MASS RENORMALIZATION

The bare mass is renormalized by tadpole contributions in equal-time (ET) quantization but not in light-front (LF) quantization. With the Lagrangian written as $\mathcal{L} = \frac{1}{2}(\partial_\mu \phi)^2 -$

TABLE I. Critical coupling values, adapted from [5], with use of a slightly different definition of the dimensionless coupling $\bar{g} = \frac{\pi}{6}g$. The first two values were computed in light-front quantization and the remainder in equal-time quantization.

Method	$\bar{g}_c$	Reported by
Light-front symmetric polynomials	1.1 ± 0.03	this work
DLCQ	1.38	Harindranath & Vary [6]
Quasi-sparse eigenvector	2.5	Lee & Salwen [7]
Density matrix renormalization group	2.4954(4)	Sugihara [8]
Lattice Monte Carlo	$2.70\begin{cases}+0.025\\-0.013\end{cases}$	Schaich & Loinaz [9]
	2.79 ± 0.02	Bosetti *et al.* [10]
Uniform matrix product	2.766(5)	Milsted *et al.* [11]
Renormalized Hamiltonian truncation	2.97(14)	Rychkov & Vitale [5]

$\frac{1}{2}\mu_0^2\phi^2 - \frac{\lambda}{4!}\phi^4$, this results in a difference that can be expressed as [3]

$$\mu^2_{\rm LF} = \mu^2_{\rm ET} + \lambda\left[\langle 0|\frac{\phi^2}{2}|0\rangle - \langle 0|\frac{\phi^2}{2}|0\rangle_{\rm free}\right]. \tag{2.1}$$

where the vacuum expectation values (VEV) of ϕ^2 resum the tadpole contributions. Here the subscript *free* indicates the VEV with zero coupling.

To calculate the VEV's, we regulate them with a point splitting by (ϵ^+, ϵ^-) and introduce a decomposition of the identity in terms of the eigenstates $|\psi_n(P)\rangle$ of the light-front Hamiltonian $\mathcal{P}^-$:

$$\langle 0|\frac{\phi^2}{2}|0\rangle \to \frac{1}{2}\langle 0|\phi(\epsilon^+,\epsilon^-)\int_0^\infty dP\sum_n |\psi_n(P)\rangle\langle\psi_n(P)|\phi(0,0)|0\rangle. \tag{2.2}$$

The operator $\phi(\epsilon^+,\epsilon^-)$ is obtained by evolving forward in light-front time $x^+ \equiv t + z$ from zero to ϵ^+, so that $\phi(\epsilon^+,\epsilon^-) = e^{i\mathcal{P}^-\epsilon^+/2}\phi(0,\epsilon^-)e^{-i\mathcal{P}^-\epsilon^+/2}$.

The necessary matrix elements for the nth bound state are

$$\langle\psi_n(P)|\phi(0,0)|0\rangle = \langle 0|\psi^*_{n1}a(P)\int\frac{dp}{\sqrt{4\pi p}}a^\dagger(p)|0\rangle = \frac{\psi^*_{n1}}{\sqrt{4\pi P}} \tag{2.3}$$

and

$$\langle 0|\phi(\epsilon^+,\epsilon^-)|\psi_n(P)\rangle = \langle 0|\int\frac{dp}{\sqrt{4\pi p}}a(p)e^{-ip\epsilon^-/2}e^{-iM_n^2\epsilon^+/2P}\psi_{n1}a^\dagger(P)|0\rangle = \frac{\psi_{n1}}{\sqrt{4\pi P}}e^{-i(P\epsilon^- + M_n^2\epsilon^+/P)/2}. \tag{2.4}$$

Similarly, for the one-particle free state, the matrix elements are

$$\langle 0|a(P)\phi(0,0)|0\rangle = \langle 0|a(P)\int\frac{dp}{\sqrt{4\pi p}}a^\dagger(p)|0\rangle = \frac{1}{\sqrt{4\pi P}} \tag{2.5}$$

and

$$\langle 0|\phi(\epsilon^+,\epsilon^-)a^\dagger(P)|0\rangle = \langle 0|\int \frac{dp}{\sqrt{4\pi p}}a(p)e^{-ip\epsilon^-/2}e^{-i\mu^2\epsilon^+/2P}a^\dagger(P)|0\rangle = \frac{1}{\sqrt{4\pi P}}e^{-i(P\epsilon^-+\mu^2\epsilon^+/P)/2}. \tag{2.6}$$

On substitution of these matrix elements, the VEV's can be written as

$$\langle 0|\frac{\phi^2}{2}|0\rangle = \frac{1}{2}\sum_n \int_0^\infty dP \frac{|\psi_{n1}|^2}{4\pi P}e^{-i(P\epsilon^-+M_n^2\epsilon^+/P)/2} \text{ and } \langle 0|\frac{\phi^2}{2}|0\rangle_{\rm free} = \frac{1}{2}\int_0^\infty dP\frac{1}{4\pi P}e^{-i(P\epsilon^-+\mu^2\epsilon^+/P)/2}. \tag{2.7}$$

With use of $1=\sum_n |\psi_{n1}|^2$, the difference can be reduced to

$$\langle 0|\frac{\phi^2}{2}|0\rangle - \langle 0|\frac{\phi^2}{2}|0\rangle_{\rm free} = \sum_n \frac{|\psi_{n1}|^2}{8\pi}\int_0^\infty \frac{dP}{P}e^{-iP\epsilon^-/2}\left[e^{-i\frac{M_n^2\epsilon^+}{2P}} - e^{-i\frac{\mu^2\epsilon^+}{2P}}\right] \tag{2.8}$$

The mass shift is then proportional to

$$\langle 0|\frac{\phi^2}{2}|0\rangle - \langle 0|\frac{\phi^2}{2}|0\rangle_{\rm free} = \sum_n \frac{|\psi_{n1}|^2}{4\pi}\left[K_0(M_n\sqrt{-\epsilon^2+i\eta}) - K_0(\mu\sqrt{-\epsilon^2+i\eta})\right], \tag{2.9}$$

where η is a convergence factor. From the asymptotic behavior of the Bessel function $K_0(z)\to -\ln(z/2)-\gamma$, we obtain

$$\langle 0|\frac{\phi^2}{2}|0\rangle - \langle 0|\frac{\phi^2}{2}|0\rangle_{\rm free} = -\sum_n \frac{|\psi_{n1}|^2}{4\pi}\ln\frac{M_n}{\mu_{\rm LF}} \equiv -\Delta/4\pi, \tag{2.10}$$

Finally, the relationship between the masses is

$$\mu^2_{\rm LF} = \mu^2_{\rm ET} - \frac{\lambda}{4\pi}\Delta \text{ or } \frac{\mu^2_{\rm ET}}{\mu^2_{\rm LF}} = 1 + g_{\rm LF}\Delta. \tag{2.11}$$

This implies coupling constant and mass ratios of

$$g_{\rm ET} = \frac{g_{\rm LF}}{\mu^2_{\rm ET}/\mu^2_{\rm LF}} = \frac{g_{\rm LF}}{(1+g_{\rm LF}\Delta)} \text{ and } \frac{M^2}{\mu^2_{\rm ET}} = \frac{1}{1+g_{\rm LF}\Delta}\frac{M^2}{\mu^2_{\rm LF}} \tag{2.12}$$

The shift Δ is plotted in Fig. 2. As the critical coupling is approached, the shift does not behave as it should. Fits are then done for coupling values much less than the critical value, in order to extrapolate. The extrapolations of the shift then yield $\Delta(g=2.1) = -0.47\pm 0.12$. The latest equal-time value for the critical coupling [5], $g_{\rm ETc} = \frac{6}{\pi}2.97 = 5.67$, implies a shift of $(g_{\rm LFc}/g_{\rm ETc}-1)/g_{\rm LFc} = -0.30$, which is consistent.

The criterion for the set of coupling values used is determined by examining the behavior of the predicted equal-time values for the mass squared, based on the relationship in (2.12), as shown in Fig. 3. Above $g=1$ the equal-time masses begin to increase rather than continue the proper decrease.

The origin of the increase in the mass, and the improper behavior of the shift near the critical coupling, is in the finiteness of the relative probabilities for higher Fock states, displayed in Fig. 4. As the critical coupling is approached there is only a continued gradual increase, implying that the one-body probability $|\psi_{11}|^2$ remains nonzero. This causes the shift Δ to diverge as the eigenmass M_1 goes to zero.

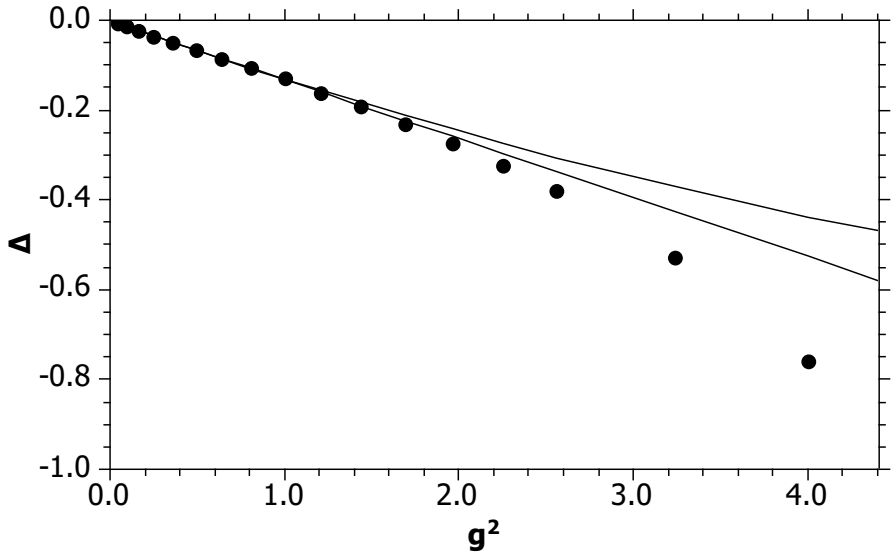

FIG. 2. The renormalization shift Δ as a function of the square of the dimensionless coupling g, as shown in [1]. The points displayed are obtained as extrapolations in the polynomial basis size. The lines are linear and quadratic fits to shifts below $g = 1$, extrapolated to the region of the critical coupling.

III. SECTOR-DEPENDENT CONSTITUENT MASS

With a sector-independent constituent mass μ, the invariant mass of a higher Fock state is quite large and such states are then naturally suppressed in any calculation with a Fock-space truncation. An obvious way to avoid this suppression is to use a sector-dependent mass [12–17] μ_m. The matrix eigenvalue problem given in [4] can then be written as

$$\sum_{n'i'} \left[\tilde{\mu}_m^2 T^{(m)\prime}_{ni,n'i'} + V^{(m,m)\prime}_{ni,n'i'}\right] c^{(m)\prime}_{n'i'} + \sum_{n'i'} V^{(m,m+2)\prime}_{ni,n'i'} c^{(m+2)\prime}_{n'i'} \tag{3.1}$$

$$+ \sum_{n'i'} V^{(m,m-2)\prime}_{ni,n'i'} c^{(m-2)\prime}_{n'i'} = \tilde{M}^2 c^{(m)\prime}_{ni}, \tag{3.2}$$

with $\tilde{\mu}_m \equiv \mu_m\sqrt{4\pi/\lambda}$ and $\tilde{M} \equiv M\sqrt{4\pi/\lambda}$. The sector-dependent mass then allows for the fact that a Fock-space truncation forces self-energy corrections to be different in each Fock sector; in particular, in the highest sector there is no self-energy correction. When the Fock-space truncation is removed, in the $N_{\max} \to \infty$ limit, the dimensionless sector-dependent mass $\tilde{\mu}_m$ becomes $\tilde{\mu} \equiv \pm 4\pi\mu^2/\lambda$. This convergence to the sector-independent mass happens first in the lowest sector; therefore, the dimensionless coupling $g \equiv \frac{\lambda}{4\pi\mu^2}$ can be extracted as $g \simeq 1/|\tilde{\mu}_1^2|$ and the dimensionless eigenmass as $M^2/\mu^2 = g\tilde{M}^2 = \tilde{M}^2/|\tilde{\mu}_1^2|$.

The sector-dependent case is no longer an explicit eigenvalue problem. The sector-dependent masses $\tilde{\mu}_m$ must be computed recursively for a given value of $\tilde{M}$ and then translated into values for g and M/μ. The recursive nature is that each $\tilde{\mu}_m$ is computed with only the Fock sectors above taken into account, by computing it in a truncation where $\tilde{\mu}_m$ is the mass in the one-body sector and the top sector has $N_{\max} - m + 2$ constituents. In the top sector, $\tilde{\mu}_{N_{\max}}$ is just $\tilde{M}$. For each sector in between, the mass $\tilde{\mu}_m$ has been computed by

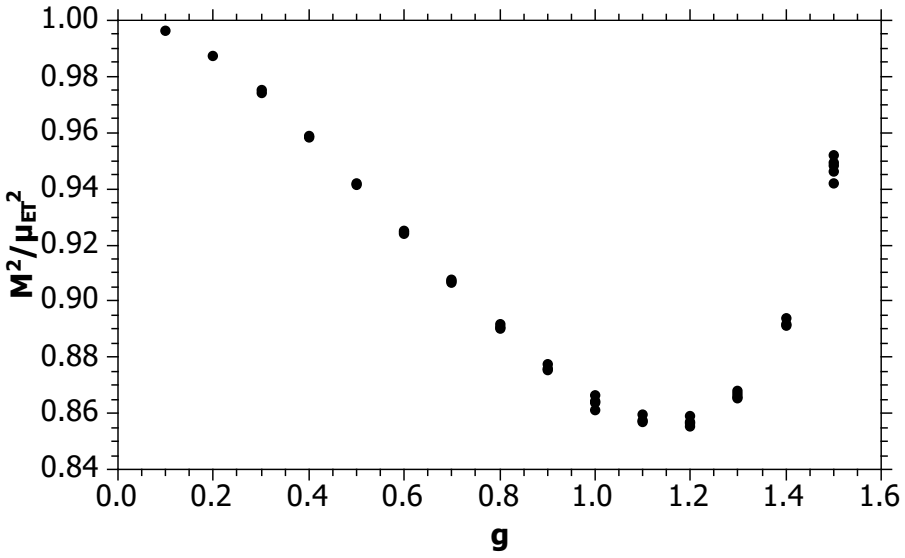

FIG. 3. Lowest equal-time mass eigenvalues for odd numbers of constituents plotted versus the dimensionless light-front coupling g, from [1]. Different points at the same g value correspond to different truncations of the polynomial basis size.

solving the smaller problem where $\tilde{\mu}_m$ was the mass in the one-body sector and the highest sector had $N_{\max} - m + 1$ constituents with mass $\tilde{M}$.

To carry out this calculation, we define set of matrices $G^{(m)}$, from $m = N_{\max}$ down to 3, as

$$G^{(m)} = \left[\tilde{\mu}_m^2 T^{(m)\prime} + V^{(m,m)\prime} - \tilde{M}^2 I^{(m)} - V^{(m,m+2)\prime} G^{(m+2)} V^{(m+2,m)\prime}\right]^{-1}, \tag{3.3}$$

$$G^{(N_{\max})} = \left[\tilde{M}^2 T^{(N_{\max})\prime} + V^{(N_{\max},N_{\max})\prime} - \tilde{M}^2 I^{(N_{\max})}\right]^{-1}. \tag{3.4}$$

The mass in the lowest sector is then simply

$$\tilde{\mu}_1^2 = \frac{1}{T^{(1)}}\left[\tilde{M}^2 - V^{(1,1)\prime} - V^{(1,3)\prime} G^{(3)} V^{(3,1)\prime}\right]. \tag{3.5}$$

The coefficients for the wave-function expansions are constructed recursively from $m = 3$ up to $N_{\max}$ by

$$\vec{c}^{\,(m)\prime}/c^{(1)} = G^{(m)} V^{(m,m-2)\prime} \vec{c}^{\,(m-2)\prime}/c^{(1)}. \tag{3.6}$$

The relative probabilities are compared with those of the sector-independent approach in Fig. 4. The sector-dependent results do converge more slowly, with respect to the Fock-space truncation, requiring $N_{\max} = 9$ to reach the convergence found at $N_{\max} = 5$ for the sector-independent calculation. The slower convergence is to be expected, and even desired, given that we expect the higher Fock states to contribute more easily and to be more important as the critical coupling is approached. However, the relative probabilities continue to show no critical behavior.

IV. SUMMARY

It is possible to understand the difference between ET and LF values of the critical coupling by taking the different mass renormalizations into account. However, calculation

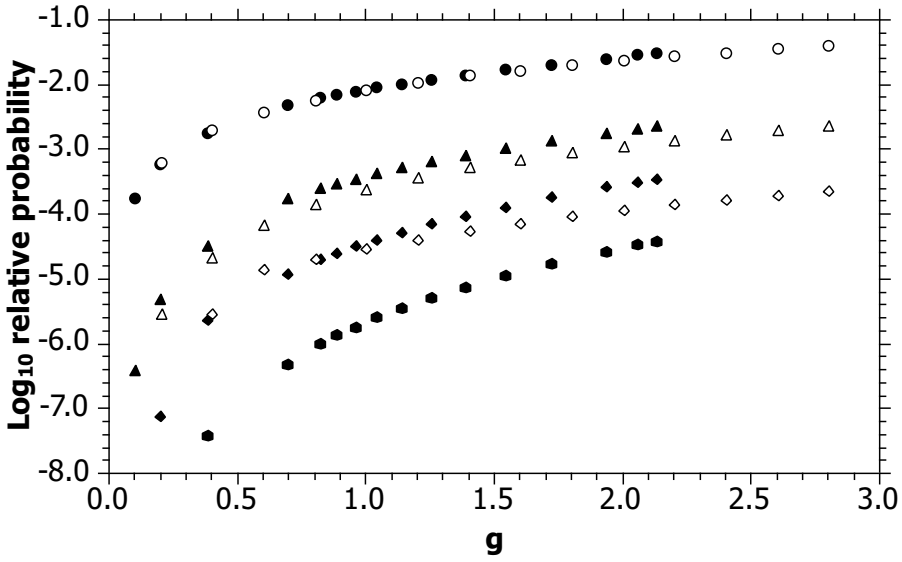

FIG. 4. Relative Fock-sector probabilities for the lowest mass eigenstate with odd numbers of constituents, for both sector-dependent (closed symbols) and independent (open symbols), with the maximum number of constituents $N_{\max} = 9$ and 7, respectively. The sectors represented include three (circles), five (triangles), seven (diamonds), and nine (hexagons) constituents.

of the mass shift near the critical coupling shows poor behavior of computed eigenstates. The relative probabilities of higher Fock states do not show critical behavior; they should diverge because the one-body probability should go to zero. The use of a sector-dependent constituent mass does not help. The difficulty near the critical coupling is avoided instead by extrapolation from smaller coupling values.

The correct representation of the eigenstates near critical coupling apparently requires a method without Fock-space truncation. In general, this would be a coherent-state basis. A specific implementation might be the light-front coupled cluster method [18] with a nontrivial valence state, such as a linear combination of the one-body and three-body states.

ACKNOWLEDGMENTS

This work was done in collaboration with M. Burkardt and J.R. Hiller, and was supported in part by the Minnesota Supercomputing Institute of the University of Minnesota with allocations of computing resources.

[1] Burkardt, M., Chabysheva, S.S., Hiller, J.R.: Two-dimensional light-front ϕ^4 theory in a symmetric polynomial basis. Phys. Rev. D **94**, 065006 (2016)

[2] Chabysheva, S.S.: Light-front ϕ^4_{1+1} theory using a many-boson symmetric-polynomial basis. Few Body Sys. **57**, 675-680 (2016)

[3] Burkardt, M.: Light-front quantization of the sine-Gordon model. Phys. Rev. D **47**, 4628-4633 (1993)

[4] J.R. Hiller, J.R.: Symmetry breaking in light-front ϕ^4 theory. in these proceedings (2016)

[5] Rychkov, S., Vitale, L.G.: Hamiltonian truncation study of the ϕ^4 theory in two dimensions. Phys. Rev. D **91**, 085011 (2015)
[6] Harindranath, A., Vary, J.P.: Solving two-dimensional ϕ^4 theory by discretized light-front quantization. Phys. Rev. D **36**, 1141-1147 (1987)
[7] Lee, D., Salwen, N.: The diagonalization of quantum field hamiltonians. Phys. Lett. B **503**, 223-235 (2001)
[8] Sugihara, T.: Density matrix renormalization group in a two-dimensional lambda ϕ^4 Hamiltonian lattice model. J. High Energy Phys. **05**, 007 (2004)
[9] Schaich, D., Loinaz, W.: An improved lattice measurement of the critical coupling in ϕ_2^4 theory. Phys. Rev. D **79**, 056008 (2009)
[10] Bosetti, P., De Palma, B., Guagnelli, M.: Monte Carlo determination of the critical coupling in ϕ_2^4 theory. Phys. Rev. D **92**, 034509 (2015)
[11] Milsted, A., Haegeman, J., Osborne, T.J.: Matrix product states and variational methods applied to critical quantum field theory. Phys. Rev. D **88**, 085030 (2013)
[12] Perry, R.J., Harindranath, A., Wilson, K.G.: Light front Tamm–Dancoff field theory. Phys. Rev. Lett. **65**, 2959-2962 (1990)
[13] Perry, R.J., Harindranath, A.: Renormalization in the light front Tamm-Dancoff approach to field theory. Phys. Rev. D **43**, 4051-4073 (1991)
[14] Hiller, J.R., Brodsky, S.J.: Nonperturbative renormalization and the electron's anomalous moment in large-α QED. Phys. Rev. D **59**, 016006 (1998)
[15] Karmanov, V.A., Mathiot, J.-F., Smirnov, A.V.: Systematic renormalization scheme in light-front dynamics with Fock space truncation. Phys. Rev. D **77**, 085028 (2008)
[16] Karmanov, V.A., Mathiot, J.-F., Smirnov, A.V.: Nonperturbative calculation of the anomalous magnetic moment in the Yukawa model within truncated Fock space. Phys. Rev. D **82**, 056010 (2010)
[17] Chabysheva, S.S., Hiller, J.R.: On the nonperturbative solution of Pauli–Villars regulated light-front QED: A comparison of the sector-dependent and standard parameterizations. Ann. Phys. **325**, 2435-2450 (2010)
[18] Chabysheva, S.S., Hiller, J.R.: A light-front coupled-cluster method for the nonperturbative solution of quantum field theories. Phys. Lett. B **711**, 417-422 (2012)